Detecting soil macrofauna using ground-penetrating radar

Melanie N. Stock[a*], David J. Hart[b], and Nicholas J. Balster[c]

[a]M.N. Stock, Utah State University, Department of Plants, Soils, and Climate, 4820 Old Main Hill, Logan, UT, 84322, USA. melanie.stock@usu.edu (email)

[b]D.J. Hart, Wisconsin Geological and Natural History Survey, 3817 Mineral Point Road, Madison, WI 53705-5100, USA. dave.hart@wgnhs.uwex.edu (email)

[c]N.J. Balster, University of Wisconsin-Madison, Department of Soil Science, 1525 Observatory Drive Madison, WI, 53706, USA. njbalster@wisc.edu (email)

*Corresponding author

Abstract

Fossorial amphibians spend up to ten months belowground, but research into this critical habitat has been impeded by a lack of noninvasive detection methods. Ground-penetrating radar (GPR), however, offers a promising tool because amphibians have theoretically strong electromagnetic (EM) contrasts relative to the soil matrix, and thus potentially high detectability. The objectives of this study were to (1) evaluate GPR by (2) experimentally-inducing three soil thermal regimes that promote stratification in the burrowing depths of 15 Eastern American Toads (*Anaxyrus americanus americanus*) during the winter of 2011–2012 in Madison, WI, USA. We calculated reflectability and established the unique electronic signature of the toads in GPR datasets through measuring the water contents of the soil and toads as a proxy for the relative dielectric constant, an EM metric in GPR assessment. As toads emerged in the spring of 2012, we verified the GPR imagery with their emergence locations. The contrast in relative dielectric constants between the toads and the soil provided reflectance ratings that were 12–24 times greater than the detectable limit and confirmed that the toads were distinguishable from other soil features. The winter mortality of the toads, however, was 73%, which limited the replication with which GPR could be evaluated. We attribute the depth and rate of frost penetration from the treatments and weather of 2012 as the probable cause of mortality. Future research and conservation efforts may be facilitated with GPR by tracking temperate species belowground and linking behavior to environmental stressors.

1. Introduction

Understanding the habits and environmental controls of fossorial amphibian families (e.g. Ambystomidae and Bufonidae) within terrestrial landscapes may help explain their enigmatic declines and elucidate new conservation efforts. The belowground environment is known to provide key refuge from fluctuations in extreme and increasingly episodic atmospheric and surface conditions, such as freezing and drought. For species of Bufonidae, however, the soil is a dominant habitat year-round (James et al. 2004). One detailed field study documented Eastern American Toads (*Anaxyrus americanus americanus*) and Great Plains Toads (*A. cognatus*) belowground for 204–207 and 230–281 days per year, respectively, in Minnesota, USA (Ewert, 1969). Once burrowed, the subsurface thermal regimes likely dictate the depth to which toads burrow and may trigger emergence (Breckenridge and Tester, 1961; Tester and Breckenridge, 1964), as the body temperature of toads (Common Toad, *Bufo bufo*) is typically within 0.2°C of the adjacent soil (vanGelder et al., 1986). From these historic studies, the subsurface environment is critical to the success of this temperate species, yet specific behavior and survival within these belowground systems remain largely unexplored.

A primary challenge to furthering terrestrial, subsurface research is a lack of noninvasive methods for monitoring amphibian behavior. For example, surgically implanted radioactive tags have been most successful for obtaining subsurface data during winter (Breckenridge and Tester, 1961; Tester and Breckenridge, 1964; Ewert, 1969). Some tagged specimens, however, exhibited abnormal behavior because of physical injury or infection from tagging procedures (Breckenridge and Tester, 1961; Ewert, 1969) and use of radioactive material (Semlitsch, 1981). Researchers have also surgically implanted radio-transmitters (vanGelder et al., 1986), but the size of these devices restricts their use to relatively large species

(Lovegrove, 2009). When externally attached (Browne and Paszkowski, 2010), the bulkiness of the radio transmitters may interfere with burrowing. Finally, the direct excavation of hibernacula were used to quantify burrowing depths (Vernberg, 1953), but this technique disturbs the soil environment and exposes the overwintering amphibians to subzero temperatures. The importance of the soil habitat to fossorial amphibians, coupled with the limitations of current methodologies, warrants a noninvasive detection technique to advance herpetological research in the subsurface environment.

In geophysical fields, ground-penetrating radar (GPR) is used to detect features without disturbing the soil profile and has shown utility in the detection of biological features, such as tree roots (Butnor et al., 2001). In principle, electromagnetic (EM) wave pulses are emitted into the soil at a selected frequency and known velocity. The pulses scatter upon contact with subsurface features that have contrasting EM properties from the surrounding substrate, causing a portion of the waves to reflect back to the GPR antenna positioned on the soil surface (Davis and Annan, 1989). By recording the velocity and the amount of time for these scattered pulses to return to the unit, the depth of the "interference" may be calculated. Therefore, the success of GPR in herpetology relies upon a sufficient contrast in EM properties between the burrowed amphibian and the surrounding soil matrix.

The most informative metric to assess EM contrasts is the relative dielectric constant, ε_r, of the targeted interference (e.g. toad) versus the soil. This unitless value describes the ability of a material to store and transmit electric fields, and increases with the water content. Using contrasts in ε_r, researchers have applied GPR to other novel settings, ranging from the detection of broad subsurface features (planar reflectors), such as changes in soil texture with depth (Kung and Lu, 1993), to distinct features (point reflectors) like tortoise burrows

(Kinlaw et al., 2007). In the case of burrowed amphibians, an abrupt EM contrast theoretically exists. The ε_r of mineral soils ranges from 6–30, depending on soil type and moisture (Bano, 2004), but is typically less than 20 (Roth et al. 1992). Conversely, a laboratory study of amphibian dielectric constants determined the ε_r of *Rana catesbieana* (bullfrogs) is 63.5 at a 1 GHz frequency (Schwartz and Mealing, 1985). Due to the apparent contrast in EM properties between most mineral soils and amphibians, GPR may offer a promising noninvasive tool to detect burrowing amphibians, such as the Eastern American Toad.

In this study, we evaluated GPR for herpetological research with overwintering toads (*A. a. americanus*) during the winter of 2011–2012. To investigate GPR detection at various depths in the soil profile, we maintained three soil thermal regimes to stratify the burrowing depths of the toads. We hypothesized that (1) toads overwintering within the coldest soil temperature treatments burrow the deepest to avoid freezing soil temperatures and (2) the ε_r of soil in this experiment would be less than 20, while the ε_r of toads would be greater than 60, providing an effective contrast to detect the toads within the top meter of soil.

2. Materials and methods

2.1. Study site and specimen selection

This research was conducted at the University of Wisconsin Arboretum, a common habitat of *A. a. americanus* in Madison, WI, USA (Wisconsin Frog and Toad Survey, 2017). We established a 20 x 20 m experimental site within the Southwest Grady Oak Savannah (lat. 43.03° N, long. 89.44°W), where the soil is classified as a sandy, mixed, mesic typic endoaquolls (Granby soil series) and the vegetation is dominated by northern red oak (*Quercus rubra*), northern pin oak (*Q. ellipsoidalis*), and burr oak (*Q. macrocarpa*) saplings.

Based on 30-year normals, the mean air temperature is -7.5°C in January and 21.7°C in July, while the mean annual precipitation is 87.6 cm (WSCO, 2017).

In October 2011, we captured 15 adult Eastern American Toads (*A. a. americanus*) with a mean snout-urostyle length (SUL) of 53.4 mm ± 5.1 (± SD) and mean wet mass of 29.1 g ± 9.3 (Table 1). From October 2011 through June 2012, the toads were individually housed in open-floor terrestrial enclosures (1 x 1 x 0.15 m). We constructed the aboveground walls of the enclosures with pine boards and made removable roofs of fiberglass screen and Velcro® to provide natural photoperiods and precipitation, as well as secure access to the toads. To minimize the potential escape of the toads and the entry of predators, we extended the walls of each enclosure to a depth of 0.5 m below the soil surface with polypropylene wildlife netting (0.635 cm mesh). For refuge, we placed a concrete cover object (0.36 x 0.18 x 0.09 m) over a small depression in the center of each enclosure (0.08 m diameter, 0.04 m depth). After releasing the toads into their enclosures in October 2011, we visually monitored the location and activity of each specimen at a minimum of every other day. Monitoring continued until no toads were observed aboveground for two weeks, at which point we presumed all to have burrowed belowground for the winter of 2011–2012.

To measure environmental conditions without interfering with the overwintering behavior of the toads, we established three instrumentation plots at the center of the site. In each plot, soil temperature was monitored every half hour at 0.10, 0.20, 0.30, 0.45, 0.60, 0.75 m depths with copper-constantan thermocouples (Type T) and a datalogger (model CR10X, Campbell Scientific Inc., Logan, UT, USA). Each plot also contained one frost tube (Rickard and Brown, 1972; Mackay, 1973), with which we monitored soil frost depth to the nearest mm at a minimum of once per week. Air temperature was measured at two-hour intervals in

the center of the site with HOBO Pendant® Temperature Data Loggers (part UA-001-08, Onset Computer Corporation, Bourne, MA, USA). At a minimum of once per week during the freezing season, we manually measured snow depth at three locations around the site.

2.2. Temperature manipulation and subsurface detection

We randomly assigned each of the 15 toads and three instrumentation plots to one of three soil thermal regimes (i.e. five enclosures and one instrumentation plot per temperature treatment) prior to the soil freezing in winter 2011 (Figure 1). To maintain differences in soil temperature, hence frost depth and potential burrowing depth, we altered the insulation on the soil surface and extended the treatments 0.5 m beyond the edge of each plot to minimize potential edge effects. The three soil thermal regimes included:

(1) "uninsulated" treatments, in which we removed snowpack within 24 hours of a precipitation event to maximize soil temperature fluctuations, soil frost depth, and potential burrowing activity;

(2) "snow-insulated" treatments, which naturally accumulated snow to dampen soil temperature fluctuations, reduce soil frost development, and potential burrowing activity;

(3) "straw-insulated" treatments, which contained 0.75 m of straw on the soil surface to test an insulated soil thermal regime in the event of a winter with low snowfall.

On 15 March 2012, we used Ground-penetrating Radar (model SIR-3000™, Geophysical Survey Systems, Inc., Nashua, NH) with a 900 MHz antenna to detect the burrowed toads. Because of the novelty in using GPR for herpetology and the unconventionally small target size of the toads, we first tested the resolution of the antenna and the theoretical contrast in electromagnetic properties between the soil and toads with a buried sponge. To represent a toad, the sponge was cut to the approximate dimensions (0.05 L x 0.05 W x 0.02 m H) and

wetted to the approximate water content (75%, by mass) of a toad. After burying the sponge at a known depth of 0.7 m in the soil, we confirmed the depth scale calculated by the GPR unit with the known depth of the buried sponge.

Prior to scanning the plots containing toads, we removed the aboveground enclosures and surface vegetation, which improves the resolution of GPR. We then placed a plywood grid (1.20 x 1.20 m, marked at 0.15 m intervals in the x- and y-directions) on the soil surface to systematically scan each plot at 0.15 m intervals in both the x- and y-directions. From this configuration, we obtained a total of 14 GPR datasets (radargrams) per plot for analysis. To account for soil textural changes within radargrams, as well as calculate the ε_r of the soil to assess the EM contrast with the toads, we collected eight soil samples from the soil surface (0.00–0.10 m) and eight samples from a 0.30–0.40 m depth, where a visible change in texture occurred. The eight soil sampling locations included: three from the instrumentation plots (i.e. one per instrumentation plot) and five randomly sampled across the field site. From these 16 samples, we measured the soil particle size distribution (Gee and Bauder, 1986), bulk density, and water content (Table 2). The mean textural class was a loamy sand at 0.00–0.10 m, underlain by a sand at 0.30–0.40 m. The average volumetric water content, θ_v, was $28 \pm$ (SD) 0.02% at 0.00–0.10 m (17% by mass) and $15 \pm 0.01\%$ at 0.30–0.40 m (9% by mass). Using the following equation (Topp et al., 1980):

$$\varepsilon_{r,soil} = 3.03 + 9.3(\theta_v) + 146.0(\theta_v^2) - 76.7(\theta_v^3) \tag{1}$$

we calculated the relative dielectric constant of the soil, $\varepsilon_{r,soil}$, to be 15.4 in the surface horizon and 7.5 below a 0.30 m depth (Table 2).

2.3. Toad Emergence and Analysis

After the aboveground enclosures were secured to their respective plots on 16 March 2012, we monitored for the emergence of the toads every two days. Upon emergence, we recorded the surface location of each exit hole (i.e. *x* and *y* coordinates), and measured the springtime length of each toad to the nearest mm and the wet mass to the nearest 0.001 g. To approximate the ε_r of the toads through water content measurements, the toads were euthanized with a 2% MS-222 (Tricaine-S) solution at pH 7 and stored at -20°C until their water content could be measured by oven-drying at 105˚C. We then compared the water content of the toads to that of bullfrogs, which have established EM properties (Schwartz and Mealing, 1985). Any enclosure from which a toad did not emerge was subsequently excavated in October 2012 to determine the belowground location of the presumably deceased toad (i.e. *x,y,z* coordinates). Excavations were completed by hand, removing each layer of soil at 1 cm intervals down to a maximum depth of 0.85 m.

2.4. Radargram Evaluation

We quantified the detectability of the toads with GPR by calculating their reflectance power, P_r, with the soil, which is the ability of a material (e.g. toad) to effectively reflect EM waves back to the GPR unit (modified from Ramo et al., 1965):

$$P_r = \left[\frac{\sqrt{\varepsilon_{r,target}} - \sqrt{\varepsilon_{r,soil}}}{\sqrt{\varepsilon_{r,soil}} + \sqrt{\varepsilon_{r,target}}} \right]^2 \qquad\qquad [2]$$

where $\varepsilon_{r,target}$ represents the relative dielectric constant of the toad, $\varepsilon_{r,soil}$ represents the relative dielectric constant of a given soil layer, and $P_r > 0.01$ is considered an effective reflecting power. Because other subsurface features within the soil profile may reflect GPR signals (e.g. textural changes with depth or buried stones), we also aimed to establish the electronic signature of the toads on reflected waveforms. First, because the toads are discrete subsurface

objects (point reflectors), their wave forms should appear as a hyperbolic shape - not broad horizontal bands - in radargrams. Second, if $\varepsilon_{r,toads} > \varepsilon_{r,\,soil}$, the polarity of the reflected wave will not be inverted, i.e. the reflected wave will maintain the same positive-negative-positive polarity within its oscillation pattern that is seen in the soil direct wave (Rial et al., 2009).

With the electronic signature of the toads predicted, we evaluated the radargrams using RADAN 7 software (Geophysical Survey Systems, Inc., Nashua, NH). Each radargram was minimally post-processed: the images were degained to remove the field gain automatically applied by the instrument and adjusted such that the horizontal distances and time zero matched the width of the plywood grid and soil surface, respectively. After the radargrams were processed, we added a display gain to highlight contrasts and identify subsurface features. For datasets in which the toads were recovered in 2012, we compared the EM reflections recorded in the GPR datasets to the locations of springtime emergence or of their excavated remains.

3. Results

3.1. Weather and Soil Thermal Regimes

The winter of 2011–2012 and spring 2012 had uncharacteristically high air temperatures and low precipitation compared to the 30-year normal (1981–2010). The mean air temperature from January 2012 – June 2012 was 5.4°C higher than the 30-year normal; March 2012 alone was 9.9˚C higher than normal (WSCO, 2017). The snow accumulation during the winter of 2011–2012 was approximately 47 cm less than the 30-year normals and by June 2012, the total precipitation was 15.6 cm lower than normal.

The uninsulated treatment resulted in the coldest soil thermal regime during the winter of 2011–2012, while the straw-insulated treatment resulted in the warmest, and the snow-

10

insulated treatment was intermediate (Figure 2). From January–March 2012, the mean daily soil temperature was -0.8 ± (SD) 1.2°C in the uninsulated treatment, -0.2 ± 0.4°C in the snow-insulated treatment, and 0.3 ± 0.3°C in the straw-insulated treatment at 0.10 m depths. Sub-freezing soil temperatures were recorded at maximum depths of 0.75 m in the uninsulated treatment, 0.30 m in the snow-insulated treatment, and 0.10 m in the straw-insulated treatment. Concurrent with the differences in soil temperature, the soil frost penetrated to a maximum depth of 0.50 m in the uninsulated treatment, 0.31 m in the snow-insulated treatment, and 0.03 m in the straw-insulated treatment (Figure 2). The soil frost thawed by 13 March 2012 in the uninsulated treatment, 15 March 2012 in the snow-insulated treatment, and 02 February 2012 in the straw-insulated treatment. The mean frost depth reached as much as 3.4 cm into the soil under the straw-insulated plots, but for less than two weeks during January 2012, concurrent with the coldest air temperatures measured during this experiment (Figure 3).

3.2. Toad Analysis and Radargram Evaluation

Between 23 March 2012 – 31 May 2012, four of the 15 toads emerged, of which three overwintered in the straw-insulated treatment, one overwintered in the uninsulated treatment, and none overwintered in the snow-insulated treatment (Table 1). Our excavation in October 2012 recovered one carcass from a straw-insulated treatment and one carcass from a snow-insulated treatment, both at depths of 0.25 m. We did not observe the emergence of the remaining toads, nor did we confirm their carcasses during the October excavation. Of the four toads that had successfully emerged, the mean springtime wet mass was 27.80 ± (SD) 6.6 g, the mean SUL was 61.5 ± (SD) 7.0 mm, and the mean water content was 80.8 ± (SD) 2.0% by mass. Because the water content of the toads was close to that established for

11

bullfrogs (79.4%), which have an established ε_r of 63.5 at 1 GhZ frequency (Schwartz and Mealing, 1985), we considered $\varepsilon_{r,toad} \sim \varepsilon_{r,bullfrog}$. We then calculated $P_r = 0.12$ for toads burrowed in the soil surface horizon ($\varepsilon_{r,soil} = 15.4$) and $P_r = 0.24$ for toads burrowed at depths greater than 0.3 m ($\varepsilon_{r,soil} = 7.5$).

From the radargram analysis, the sponge test object was detected by GPR at depth of 0.71 m and it exhibited a hyperbolic shape (the signature of a point reflector) with maintained polarity (the signature of a feature with a higher ε_r, or water content, than the surrounding soil) (Figure 4). Of the four toads that emerged in spring 2012, toads 10 (straw-insulated treatment), 11 (straw-insulated treatment), and 13 (uninsulated treatment) were likely detected, but toad 12 (straw-insulated treatment) was not (Table 3). An example of an interference attributed to a toad (i.e. an interference with a hyperbolic shape and no inversion of polarity) can be seen in Figure 5. Of the three potentially detected toads, two exhibited a strong hyperbolic shape within the radargrams and three of the four that emerged reflected waveforms in which the polarity was not inverted (i.e. a positive-negative-positive pattern was maintained). False positives were not observed in the radargrams and the two deceased toads that were recovered in October 2012 were not detected with GPR.

4. Discussion

Ground-penetrating radar at a 900 MHz frequency provided nondestructive, subsurface detection of three of the four toads that emerged in the spring of 2012, as well as the buried sponge that was sized and wetted to mimic the EM properties of the toads in this experiment. Through measuring the water contents of the toads and soil to calculate Pr, we confirmed a strong and abrupt contrast in dielectric constants exists, exceeding the detection limit by 12 times in the surface horizon and 24 times in the subsurface horizon. Therefore, living toads

are theoretically detectable at any depth within the top meter of this soil profile. Deceased toads, however, were not detected by GPR or recovered in excavations, presumably because of their rapid decay rate (0.062 d^{-1}) (Regester and Whiles, 2006). We also determined the electronic signature of the living toads is a hyperbolic shape with a lack of polarity inversion in the reflected waveform, evidenced by both measuring water content as a proxy for the dielectric constant and ground-truthing the radargrams with emergence locations. The electronic signatures observed in this study present GPR as a method for the research of toads or other burrowed herptile species with similar water contents, as they were distinguishable from other point reflectors in the soil, such as rocks, which invert waveform polarity. By creating 3D radargrams from the x- and y-direction scans of the enclosures, the toads were also distinguishable from tree roots, which have relatively high water contents, but are not discrete point reflectors.

Because one of the four emerged toads was not detected with GPR, we recommend increasing the frequency of the antenna to improve the resolution, hence consistency, of GPR detection in similar applications. At 900 MHz, GPR has a vertical resolution of 0.02 m and a horizontal resolution of a 0.04 m^2 area in our soil profile (Reynolds, 2011). Smaller or vertically-oriented amphibians may be more consistently detected with a 2600 MHz antenna, which has a vertical resolution of 0.007 m and horizontal resolution of a 0.01 m^2 area. Increasing the antenna frequency, however, limits the depth of GPR penetration, as a 900 MHz antenna detects down to 1 m in this soil profile, while a 2600 MHz antenna penetrates to a depth of 0.4 m (GSSI, 2016). Another consideration in optimizing the resolution and penetration depth of GPR is soil texture. We conducted our study in a uniform loamy sand to sand soil habitat, which was ideal for the transmission of wave pulses. In soils with a high

clay content ($> 35\%$), wave pulses tend to attenuate, which decreases the penetration depth of any GPR antenna (Doolittle and Collins, 1995). Therefore, in addition to the soil texture of a given site, a tradeoff between resolution and penetration depth must be considered when using GPR for similar applications.

The low emergence rates of the toads limited the replication with which we could evaluate GPR and highlighted the importance of wintertime controls on population dynamics. As three of the four survived toads overwintered in the straw-insulated treatment, we attribute the depth and rate of frost penetration in both the uninsulated and snow-insulated treatments to be the most probable cause of high mortality. For example, the remains of toad 8, which overwintered in an uninsulated treatment, were recovered at a depth of 0.25 m, half of the maximum frost depth (0.50 m). The frost advancement from 0.23 to 0.42 m at a rate of 0.06 m d^{-1} during the coldest air temperatures (18–21 January 2012) may have outpaced the burrowing toads, which exhibit reduced muscle force at low temperatures (Johnston and Gleeson 1987). We also speculate the burrowing limits of the toads were reached in the snow-insulated plot, as the mild and droughty weather reduced snow accumulation, thereby accelerating frost development (e.g. 0.03 m d^{-1} during 12–14 February 2012, when frost advanced from 0.21 to 0.28 m). Meanwhile, the straw-insulated plots mimicked winters with continuous, heavy snowpack, whereby the toads experienced a thermally-stable subsurface habitat with reduced burrowing demands, and perhaps even incurred lower energetic costs (Reading, 2007). In a similar experimental design, the survival rate of freeze-tolerant Wood Frogs (*Lithobates sylvaticus*) was four times higher in snow-insulated versus uninsulated enclosures (O'Conner and Rittenhouse, 2016), supporting the control of soil freezing dynamics on wintertime survival.

Linking the subsurface behavior of temperate amphibians to abiotic conditions, as well as quantifying species-specific mortality rates, may further identify susceptibility to environmental stressors. The winter mortality rates of *A. a. americanus* were 73% across all treatments in this study, though the straw-insulated treatment (25%) was comparable to the 32% of *A. a. americanus* that did not survive under continuous snowpack ranging from 0.15—0.61 m deep in Minnesota (Ewert, 1969). The documented winter mortality rates of other species of toads are also relatively high, though may relate to maturity: 89% for juvenile *Incilius valliceps* (Blair, 1953), 70–78% for juvenile *A. fowleri* (Clarke, 1977), 80–99% for juvenile *Bufo viridis* and 59–95% for *Epidalea calamita* (Sinsch and Schäfer, 2016), 67% for adult *A. cognatus* (Ewert, 1969), 28–62% for adult *E. calamita* (Stephan et al., 2001), and 40–65% for adult *B. viridis* (Sinsch et al., 2007). While the toads in this study were not directly aged, the SUL and mass of the surviving toads – including Toad 13, which emerged from an uninsulated plot – were among the largest. We speculate the greater body size of the surviving toads may have improved their ability to burrow and escape freezing soil temperatures, also aiding winter survival (Sinsch and Schäfer, 2016).

We have shown the difference in EM properties between the Eastern American Toads and the soil provides a strong contrast to reflect GPR wave pulses and demonstrates the use of GPR for herpetological research. The most common EM metric to assess GPR detectability in novel settings is relative dielectric constant, which is largely a function of water content. Live amphibians have a significantly greater water content than most other subsurface features and may be distinguished from other point reflectors in the soil profile. The tradeoffs in resolution and detection depth of GPR, the size of the targeted amphibian, its burrowing depth, and the soil type must be considered. The elevated mortality rates of the toads in this study (i.e. low

replication) limited our evaluation of GPR and underscores the role of soil physical properties and snowpack on overwintering success. By furthering the development of GPR in herpetology, we may better understand the fate and interactions of fossorial amphibians with this vital subsurface habitat.

References

Bano, M. 2004. Modeling of GPR waves for lossy media obeying a complex power law of frequency for dielectric permittivity. Geophys. Prospect. 52:11–26.

Blair, W.F. 1953. Growth, dispersal and age at sexual maturity of the Mexican Toad (*Bufo valliceps Wiegmann*). Copeia. 1953(4):208–212.

Breckenridge, W.J. and J.R. Tester. 1961. Growth, local movements, and hibernation of the Manitoba Toad, *Bufo hemiophrys*. Ecology. 42 (4):637–646.

Browne, C.L. and C.A. Pazkowski. 2010. Hibernation sites of western toads (*Anaxyrus boreas*): characterization and management implications. Herpetol. Conserv. Bio. 5(1):49–63.

Butnor, J.R., J.A. Doolittle, L. Kress, S. Cohen, and K.H. Johnsen. 2001. Use of ground-penetrating radar to study tree roots in southwestern United States. Tree Physiol. 21:1269–1278.

Clarke, R.D. 1977. Postmetamorphic survivorship of Fowler's Toad, *Bufo woodhousei*. Copeia. 1977(3):594–597.

Davis, J.L. and A.P. Annan. 1989. Ground-penetrating radar for high-resolution mapping of soil and rock stratigraphy. Geophys. Prospect. 37:531–551.

Doolittle, J.A. and M.E. Collins. 1995. The use of soil information to determine application of ground-penetrating radar. J. Appl. Geophys. 33:101–108.

Ewert, M.A. 1969. Seasonal movements of the toads *Bufo americanus* and *B. cognatus* in Northwestern Minnesota. Ph.D. Dissertation. University of Minnesota, Minneapolis, Minnesota. 193 p.

Gee, G.W., and J.W. Bauder. 1986. Particle-size analysis. Pp. 383–411 *In* Methods of Soil Analysis: Part 1-Physical and Mineralogical Methods. 2nd Ed. Klute, A. (Ed.). American Society of Agronomy and Soil Science Society of America, Madison, Wisconsin, USA. doi:10.2136/sssabookser5.1.2ed.c15.

Geophysical Survey Systems, Incorporated (GSSI). 2017. Antennas. Available from www.geophysical.com/antennas.htm. Accessed 17 April 2017.

James, S.M., E.E. Little, and R.D. Semlitsch. 2004. The effect of soil composition and

hydration on the bioavailability and toxicity of cadmium to hibernating juvenile

American toads (*Bufo americanus*). Environ. Pollut. 132:523–532.

Johnston, I.A. and T.T. Gleeson. 1987. Effects of temperature on contractile properties of

skinned muscle fibers from three toad species. Am. J. Physiol.–Reg. I 252(2):R273–

R275.

Kinlaw, A.E. 2007. Use of ground-penetrating radar to image burrows of the gopher tortoise

(*Gopherus polyphemus*). Herpetol. Rev. 38(1):50–55.

Kung, K.-J.S. and Z.-B. Lu. 1993. Using Ground-Penetrating Radar to detect layers of

discontinuous dielectric constant. Soil Sci. Soc. Am. J. 57:335–340.

Lovegrove, B.G. 2009. Modification and miniaturization of Thermochron iButtons for

surgical implantation into small animals. J. Comp. Physiol. B. 179:451–458.

MacKay, J.R. 1973. A frost tube for the determination of freezing in the active layer above

permafrost. Can. Geotech. J. 10:392–396.

O'Conner, J.H. and T.A.G. Rittenhouse. 2016. Snow cover and late fall movement influence

wood frog survival during an unusually cold winter. Oecologia. 181:635–644.

Ramo, S., J.R. Whinnery, and T. vanDuzer. 1984. Fields and Waves in Communication

Electronics. 2nd Ed. John Wiley & Sons, New York, New York, USA.

Reading, C.J. 2007. Linking global warming to amphibian declines through its effects on the

female body condition and survivorship. Oecologia. 151:125–131.

Regester, K.J. and M.R. Whiles. 2006. Decomposition rates of salamander (*Ambystoma

maculatum*) life stages and associated energy and nutrient fluxes in ponds and adjacent

forest in southern Illinois. Copeia. 2006(4):640–649.

Reynolds, J.M. 2011. An Introduction to Applied and Environmental Geophysics. 2nd Edition. Wiley-Blackwell. Chichester, West Sussex, England.

Rial, F.I., H. Lorenzo, M. Pereira, and J. Armesto. 2009. Waveform analysis of UWB GPR antennas. Sensors. 9(3):1454–1470.

Rickard, W. and J. Brown. 1972. The performance of a frost-tube for the determination of soil freezing and thawing depths. Soil Sci. 113(2):149–154.

Roth, C.H., M.A. Malicki, and R. Plagge. 1992. Empirical evaluation of the relationship between soil dielectric constant and volumetric water content as the basis for calibrating soil moisture measurements by TDR. J. Soil Sci. 43:1–13.

Schwartz, J.-L. and G.A.R. Mealing. 1985. Dielectric properties of frog tissue in vivo and in vitro. Phys. Med. Biol. 30(2):117–124.

Semlitsch, R. D. 1981. Effects of implanted Tantalum-182 wire tags on the mole salamander, *Ambystoma talpodeum*. Copeia. 1981(3):735–737.

Sinsch, U., C. Leskovar, A. Drobig, A. König, and W.R. Grosse. 2007. Life-history traits in Green Toad (*Bufo viridis*) populations: indicators of habitat quality. Can. J. Zool. 85:665–673. doi:10.1139/Z07-046.

Sinsch, U. and A.M. Schäfer. 2016. Density regulation in toad populations (*Epidalea calamita, Bufotes viridis*) by differential winter survival of juveniles. J. Therm. Biol. 55:20–29.

Stephan, T., K. Ulrbrich, W.R. Grosse, and F. Meyer. 2001. Modelling the extinction risk of isolated populations of the Natterjack Toad *Bufo calamita*. Web Ecol. 2:47–56.

Tester, J.R. and W.J. Breckenridge. 1964. Population Dynamics of the Manitoba Toad, *Bufo hemiophrys*, in Northwestern Minnesota. Ecology. 45(3):592–601.

Topp, G.C., J.L. Davis, and A.P. Annan. 1980. Electromagnetic determination of soil water content: measurements in coaxial transmission lines. Water Resour. Res. 16(3):574–582.

vanGelder, J.J., J.H.J. Olders, J.W.G. Bosch, and P.W. Starmans. 1986. Behaviour and body temperature of hibernating common toads *Bufo bufo*. Holarctic Ecol. 9:225–228.

Vernberg, F.J. 1953. Hibernation studies of two species of salamanders, *Plethodon cinereus cinereus* and *Eurycea bislineata bislineata*. Ecology. 34(1):55–62.

Wisconsin Frog and Toad Survey. 2017. American Toad. Available from: http://wiatri.net/inventory/frogtoadsurvey/SurveyInfo/anMapAll.cfm. Accessed 07 November 2017.

Wisconsin State Climatology Office (WSCO). 2017. Madison Climate. Available from: www.aos.wisc.edu/~sco/clim-history/7cities/madison.html. Accessed 17 April 2017.

Table 1. The snout-urostyle length, SUL, [mm] and wet mass [g] of the fifteen toads before (Fall 2011) and after (Spring 2012) overwintering, in one of three soil thermal treatments: uninsulated, snow-insulated, and straw-insulated. The Recovery Date in 2012 denotes the date the toad emerged from the soil profile (March–May 2012) or that the carcass of the toad was recovered upon excavation in October 2012.

Toad ID	Soil Thermal Treatment	Fall 2011		Spring 2012		Recovery Date in 2012
		SUL [mm]	Mass [g]	SUL [mm]	Mass [g]	
1	uninsulated	49	22.78	-	-	-
2	snow-insulated	56	35.08	-	-	-
3	straw-insulated	51	25.32	-	-	-
4	uninsulated	55	27.22	-	-	-
5	snow-insulated	54	27.81	-	-	-
6	snow-insulated	54	23.51	-	-	-
7	snow-insulated	48	20.42	-	-	-
8	straw-insulated	47	17.35	-	-	October excavation
9	snow-insulated	47	20.13	-	-	-
10	straw-insulated	50	23.80	55	18.60	Emerged 29 March
11	straw-insulated	63	54.21	71	33.04	Emerged 31 May
12	straw-insulated	58	35.56	58	27.66	Emerged 23 March
13	uninsulated	57	36.86	62	32.07	Emerged 22 May
14	uninsulated	53	30.55	-	-	-
15	uninsulated	62	35.33	-	-	October excavation

Table 2. The soil textural classes with mean (± SD) percentages of sand, silt, and clay

particle separates; bulk density, ρ_b, in g cm^{-3}; volumetric water content, θ_v, in m^3 m^{-3}; relative

dielectric constant, $\varepsilon_{r,soil}$; and reflectance power, P_r, by depth in m.

Depth [m]	Soil Texture	Sand [%]	Silt [%]	Clay [%]	ρ_b [g cm^{-3}]	θ_v [m^3 m^{-3}]	$\varepsilon_{r,soil}$	P_r
0.00–0.10	loamy sand	86.8 (± 3.6)	7.1 (± 1.5)	6.1 (± 3.9)	1.60 (± 0.06)	0.28 (± 0.02)	15.4	0.12
0.30–0.40	sand	89.5 (± 1.3)	5.9 (± 1.3)	4.6 (± 1.3)	1.76 (± 0.04)	0.15 (± 0.02)	7.5	0.24

Table 3. Characteristics of the GPR reflections from the test sponge and burrowed toads on 15 March 2012, including the field coordinates in which the sponge or toads were observed, the coordinates determined by GPR, and the waveform patterns (electronic signature) of the subsurface features.

| Toad ID	Soil Thermal Treatment	Field coordinates (x,y,z) [m]	Detected coordinates (x,y,z) [m]	Waveform Pattern	
				Shape	Polarity
NA - sponge		(1.0, 0.80, 0.75)	(1.06, 0.83, 0.71)	hyperbola	no inversion (+ - +)
10	straw-insulated	(0.73, 0.27)	(0.76, 0.37, 0.07)	hyperbola	no inversion (+ - +)
11	straw- insulated	(0.50, 0.39)	(0.58, 0.31, 0.29)	weak	no inversion (+ - +)
12	straw- insulated	(0.22, 0.40)	(0.15, 0.40, 0.31)	not detected	not detected
13	uninsulated	(0.20, 0.90)	(0.21, 0.91, 0.12)	hyperbola	no inversion (+ - +)
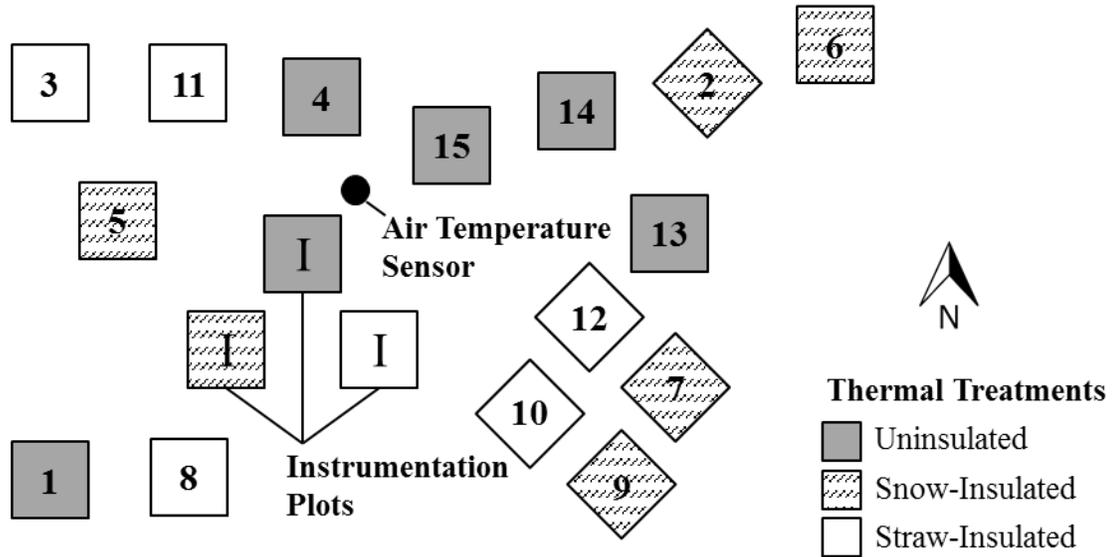
Figure 1. A diagram of the plot layout by soil insulation treatment (Uninsulated, Snow-Insulated, and Straw-Insulated) at the University of Wisconsin Arboretum in Madison, WI, USA. The numbers denote the identification number of the toad assigned to each plot and "I" denotes the instrumentation plots. Diagram not drawn to scale.
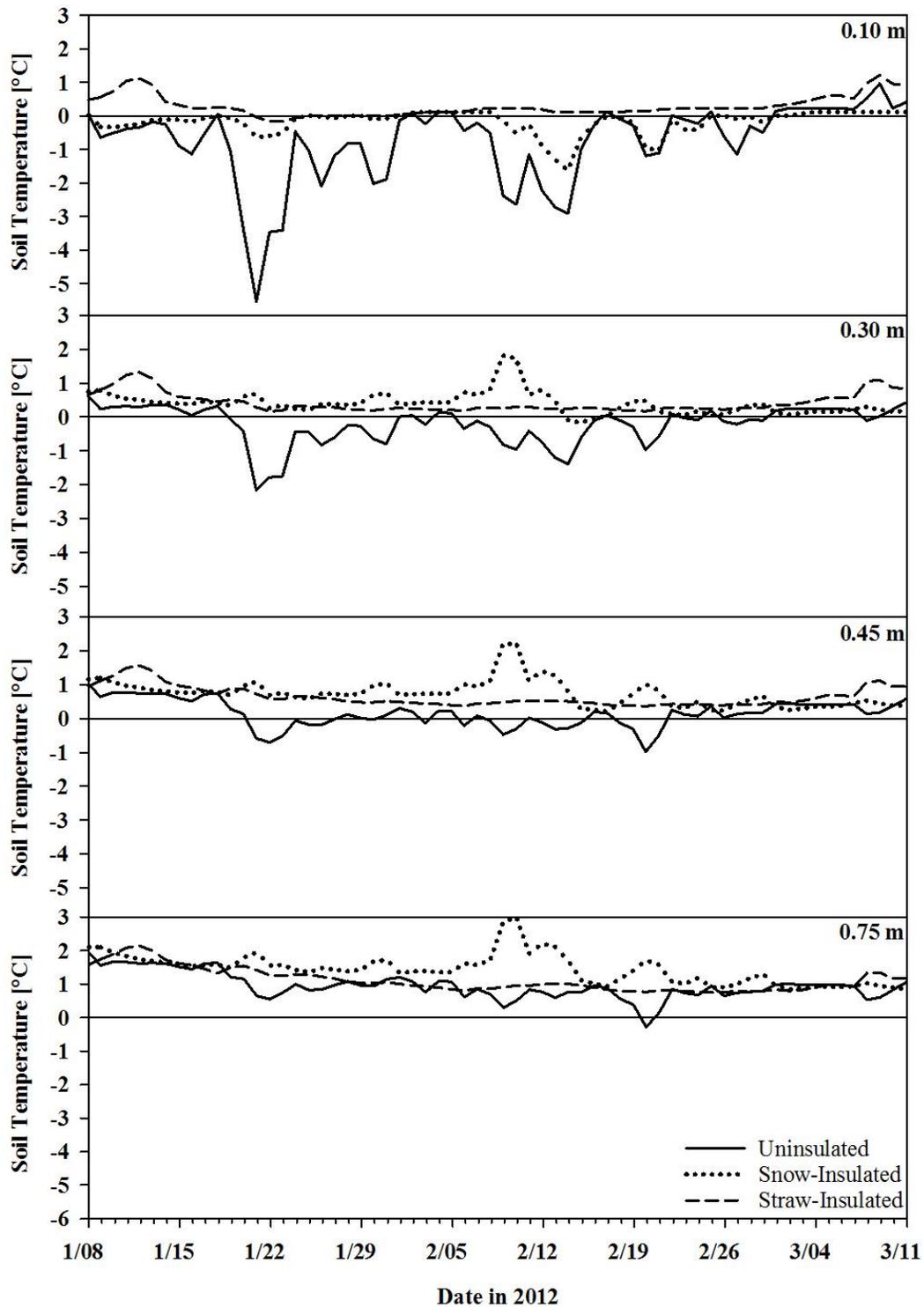
Figure 2. The mean daily soil temperature [°C] at 0.10, 0.30, 0.45, and 0.75 m depths by soil

insulation treatment (Uninsulated, Snow-Insulated, and Straw-Insulated) during January–
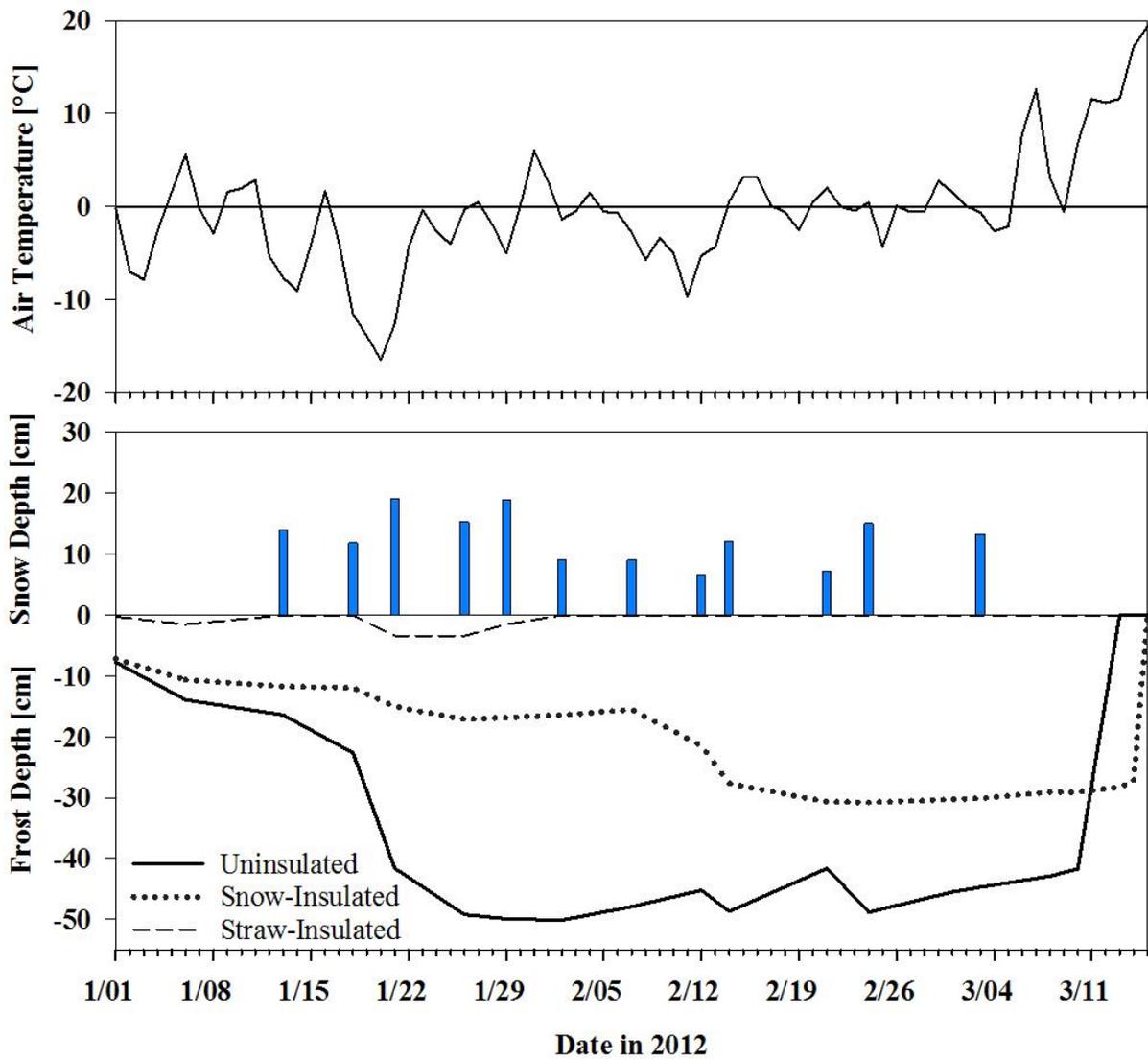
March 2012.

Figure 3. (A) Mean daily air temperature [°C] and (B) snow accumulation [cm] during the

winter of 2011–2012, with frost depth [cm] by soil insulation treatment (Uninsulated, Snow-
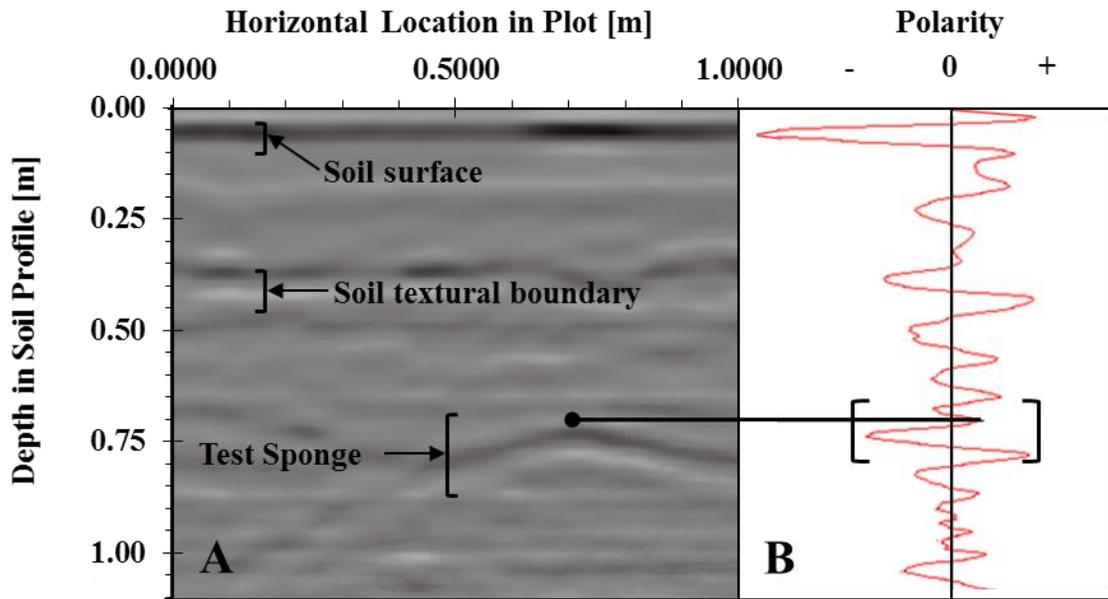
insulated, and Straw-insulated).

Figure 4. A radargram of the test sponge in the soil profile, displayed as A) LineScan (Gain = 6) and as B) Trace imagery. The black dot in the LineScan labels the top the reflection presumably caused by the sponge, which exhibits the hyperbolic shape of a point reflector. The bracketed waveform in the Trace refer to the corresponding waveform pattern in the Linescan. The Trace shows a positive-negative-positive pattern (no inversion) from the reflection, indicating the relative dielectric constant (hence water content) of the sponge was greater than that of the surrounding soil matrix. Other designated features of interest include planar reflections from the soil surface and a confirmed textural boundary at 0.30 m.
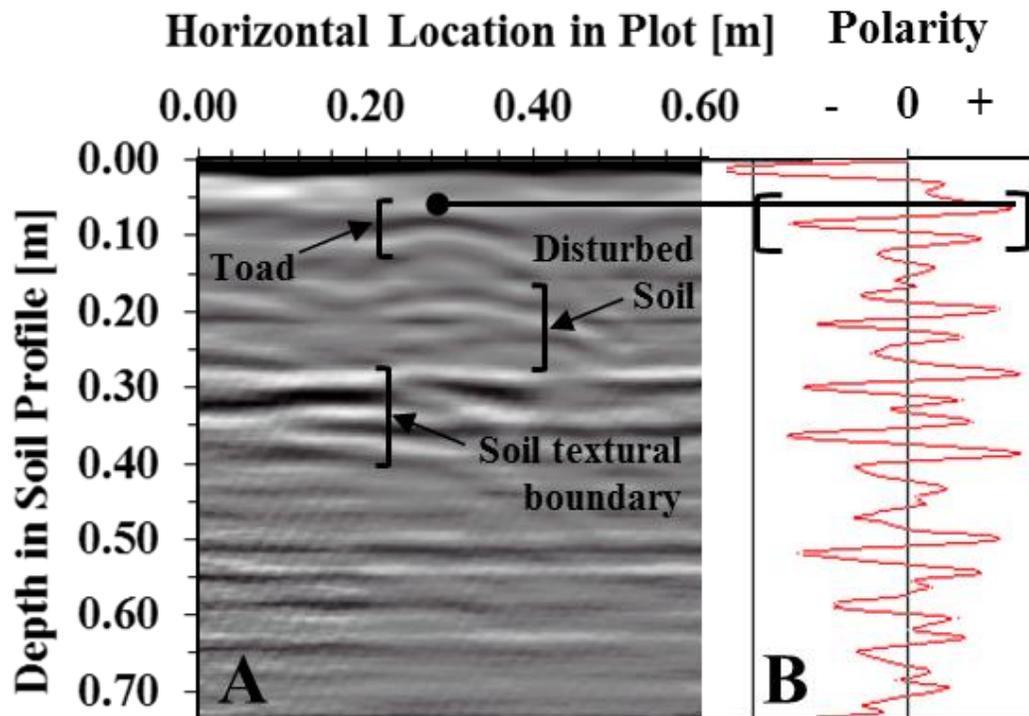
Figure 5. A radargram of Toad #10 burrowed in the soil profile of a straw-treatment, as displayed as A) LineScan (Gain = 6) and B) Trace imagery. GPR was used on 15 March 2012, and the presumed reflection of the toad was detected at coordinates (0.76 m, 0.37 m, 0.07 m) in radargram, where a hyperbolic shape and positive-negative-positive polarity pattern were observed. Toad #10 emerged on 29 March 2012, at the coordinates (0.78 m, 0.35 m). Other designated features of interest include planar reflections at the soil surface, a textural change at a 0.3 m depth, and disturbed soil below the presumed toad, perhaps from burrowing action.